Transparent Time-Delayed Bilateral Teleoperation Using Wave Variables

A. Aziminejad, M. Tavakoli, R. V. Patel, and M. Moallem

***Abstract*—Besides stability, a high degree of transparency is also an essential requirement in order to enable operators to safely and precisely perform bilateral teleoperation tasks. An existing approach based on the wave transformation technique can make a two-channel teleoperation system insensitive to time delays by making the time-delayed communication channel passive. In this paper, we propose a novel method for incorporating this technique in a four-channel architecture, which is the optimal architecture from a transparency point of view, and derive the corresponding absolute stability condition. It is analytically demonstrated that the proposed teleoperation architecture is capable of providing ideal transparency when transmission delays are present, and criteria for its stable operation are derived. We also show that a three-channel variant of the proposed four-channel control architecture can offer a comparable performance with less implementational complexity. Experimental results in support of the developed theory are provided.**

***Index Terms*—Bilateral teleoperation, passivity, time-delay compensation, transparency, wave variables.**

I. Introduction

MASTER–SLAVE teleoperation is greatly enhanced if some form of kinesthetic feedback about interaction occurring between the slave robot and the remote environment is provided to the human operator through the master robot. Such systems are called "bilateral" because information flows in two directions between the operator and the remote environment. However, communication latencies exist if there is a large distance between the local and the remote sites. Such a delayed kinesthetic feedback can pose serious problems to a bilateral teleoperation system [1]–[3]. A comprehensive survey of the literature on time-delay compensation methods can be found in [4] and [5]. The passivity-based approach has been shown to be an efficient method for stabilizing a two-channel (2CH) teleoperation architecture (involving transmission of only one quantity from the master to the slave and *vice versa*) independent of transmission delays at the expense of degraded transparency [6]. A reformulation of this idea led to the introduction of the wave transformation approach [7], [8], which provides a flexible design and analysis tool for 2CH teleoperation systems. On the other hand, it has been demonstrated that the extra "degrees of freedom" (control parameters) in the four-channel (4CH) architecture make it the best teleoperation system from a transparency point of view when there are no time delays [9], [10]. However, the problem of stabilization of the 4CH architecture under time delay without imposing any additional penalty on the system transparency has not been addressed. The main contributions of this paper are as follows.

1) A new 4CH architecture is proposed which uses wave transformation to make the delayed communication channel passive. In order to incorporate wave theory in the 4CH bilateral control architecture, we have introduced appropriate linear combinations of forces and velocities at the input and output of the delayed communication channel (that has been made passive) such that the corresponding pseudo-power signals comply with passivity formalism.
2) The passivity and absolute stability (stability of the teleoperation system coupled to an environment and an operator which are both passive but otherwise arbitrary) of the proposed wave-based 4CH architecture is rigorously studied and the corresponding condition is derived.
3) The proposed architecture is sufficiently flexible to achieve ideal transparency in the presence of time delay. We derive the conditions for realizing this property. Moreover, we conduct a stability study for the ideally transparent system and derive the stability condition.
4) We propose wave-based three-channel (3CH) architectures, which are derived from the 4CH architecture through appropriate selection of control gains. The cited bilateral teleoperation control architectures are capable of offering satisfactory suboptimal transparency with significantly less implementation complexity.

The theoretical work presented here is supported by experimental results based on a haptic teleoperation test-bed for minimally invasive surgery.

II. Preliminaries

A. System Modeling and Transparency

Fig. 1 shows an equivalent circuit representation of a bilateral teleoperation system, where Z_h, $Z_t = F_h/V_m$, Z_r, and $Z_e = F_e/V_s$ are the operator's hand impedance, the impedance transmitted to and felt by the operator, the impedance perceived by the remote environment, and the environment impedance interacted with the robot's end-effector, respectively. Also, F_h' is the exogenous hand force, F_h and F_e are the operator/master and the slave/environment interaction forces, and V_m and V_s are

Manuscript received March 9, 2007. Manuscript received in final form June 20, 2007. Recommended by Associate Editor Z. Wang. This work was supported in part by the Natural Sciences and Engineering Research Council (NSERC) of Canada under Grant RGPIN-1345 and Grant RGPIN-227612, the Ontario Research and Development Challenge Fund under Grant 00-May-0709 and infrastructure grants from the Canada Foundation for Innovation awarded to the London Health Sciences Centre (CSTAR) and the University of Western Ontario.

A. Aziminejad and R. V. Patel are with the Department of Electrical and Computer Engineering, University of Western Ontario, London, ON N6A 5B9, Canada, and also with Canadian Surgical Technologies and Advanced Robotics (CSTAR), London, ON N6A 5A5, Canada (e-mail: aazimin@uwo.ca; rajni@eng.uwo.ca).

M. Tavakoli is with the School of Engineering and Applied Sciences, Harvard University, Cambridge, MA 02138 USA (e-mail: tavakoli@seas.harvard.edu).

M. Moallem is with the School of Engineering Science, Simon Frasier University, Surrey, BC V3T 0A3, Canada (e-mail: mmoallem@sfu.ca).

Color versions of one or more of the figures in this paper are available online at http://ieeexplore.ieee.org.

Digital Object Identifier 10.1109/TCST.2007.908222

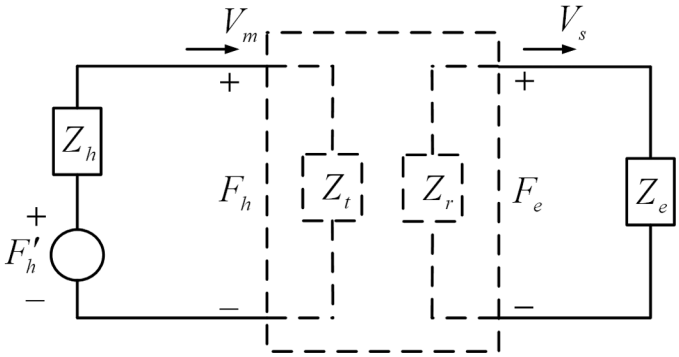

Fig. 1. Equivalent circuit representation of a bilateral teleoperator.

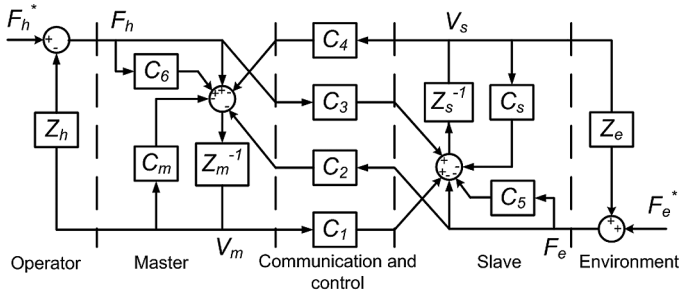

Fig. 2. 4CH bilateral teleoperation system without time delay.

the master and the slave robots velocities in the s-domain. The system in Fig. 1 can be represented by its hybrid model as

$$\begin{bmatrix} F_h \\ -V_s \end{bmatrix} = \begin{bmatrix} h_{11} & h_{12} \\ h_{21} & h_{22} \end{bmatrix} \begin{bmatrix} V_m \\ F_e \end{bmatrix}. \tag{1}$$

To achieve ideally transparent bilateral teleoperation system in the presence of time delay, the concept of transparency in [9] and [11] can be further extended to the delayed kinematic correspondence and the delayed interaction force correspondence ($V_s = e^{-sT}V_m$ and $F_h = e^{-sT}F_e$, respectively). Consequently, the corresponding hybrid matrix takes the following form:

$$H_{\text{ideal}} = \begin{bmatrix} 0 & e^{-sT} \\ -e^{-sT} & 0 \end{bmatrix}. \tag{2}$$

Throughout this paper, we assume the following equations of motions for a single-DOF master–slave teleoperation system:

$$f_h - f_m = M_m \ddot{x}_m; \quad -f_e + f_s = M_s \ddot{x}_s \tag{3}$$

where f_m and f_s are the control actions at the master and slave sides, respectively. In this system, impedances of the single-DOF master and slave robots can be represented as $Z_m = M_m s$ and $Z_s = M_s s$, respectively.

B. Wave Transformation and Scattering Theory

The wave variable approach for time-delay compensation in bilateral teleoperation stems from scattering theory and theoretically guarantees stability under arbitrary fixed time delays. The original wave transformation method proposed in [7] for a 2CH teleoperation architecture encodes the power variables velocity and force $(\dot{x}, f)$ pretransmission, as wave variables u and v. The corresponding transformation at the master side is defined as

$$u_m = (b\dot{x}_m + f_{md})/\sqrt{2b}; \quad v_m = (b\dot{x}_m - f_{md})/\sqrt{2b} \tag{4}$$

where b denotes the characteristic wave impedance, which is a positive constant. Upon arrival at the slave side, velocity and force information are extracted from the received wave variables. The slave-side post-reception transformation is

$$u_s = (b\dot{x}_{sd} + f_s)/\sqrt{2b}; \quad v_s = (b\dot{x}_{sd} - f_s)/\sqrt{2b}. \tag{5}$$

A major implementation drawback of the wave transformation approach is the wave reflection phenomenon, which can lead to oscillatory behavior. Two remedies proposed for this problem are the impedance matching procedure and the low-pass filtering in the wave domain, with low-pass filtering shown to be a more efficient solution [7], [12]. In this study, in order to overcome the reflections of the wave transformation approach in practical implementation, we use first-order low-pass filters $W(s) = (Ls+1)^{-1}$ in the wave domain, where $L = (2\pi f_{\text{cut}})^{-1}$ and f_{cut} is the cutoff frequency.

Scattering theory is a very powerful tool for stability analysis of two-port networks. For an LTI two-port network with the effort (i.e., voltage/force) vector $F = [F_m\ F_s]^T$ and the flow (i.e., current/velocity) vector $V = [V_m\ V_s]^T$, the scattering matrix is defined as

$$F - V = S(s)(F + V) \tag{6}$$

where the flow is entering the system ports and the effort is measured across the system ports. The necessary and sufficient condition for absolute stability in a reciprocal two-port network with a scattering matrix $S(s)$, which is analytic over the closed right half-plane (RHP), is [13], [14]

$$\bar{\sigma}\left[S(s)\right] \leq 1 \tag{7}$$

where $\bar{\sigma}$ represents the maximum singular value of S. In the case of a general two-port network, the passivity condition (7) is only a sufficient condition for absolute stability.

C. 4CH Architecture

Fig. 2 depicts a general 4CH bilateral teleoperation architecture [9], [10]. The operator and environment exogenous forces F_h' and F_e' are inputs independent of teleoperation system behavior. This architecture can represent all teleoperation structures through appropriate selection of subsystem dynamics C_1 to C_6. In contrast to 2CH architectures, a sufficient number of parameters (degrees of freedom) in the 4CH architecture enables it to achieve ideal transparency. The local force feedback compensators C_5 and C_6 improve stability and performance of the

system [11], [15]. In the absence of time delay, perfect transparency is achieved if and only if the hybrid matrix in (1) has the following form:

$$H = \begin{bmatrix} 0 & 1 \\ -1 & 0 \end{bmatrix} \tag{8}$$

which has been obtained from (2) by taking $T = 0$. Applying the perfect transparency conditions (8) to the hybrid parameters of Fig. 2, the following ideal transparency condition set is derived for the 4CH architecture [9], [11]:

$$C_1 = Z_{ts}; \quad C_2 = 1 + C_6; \quad C_3 = 1 + C_5; \quad C_4 = -Z_{tm} \tag{9}$$

where $Z_{tm} = M_m s + C_m(s) = M_m s + k_{dm} + k_{pm}/s$ and $Z_{ts} = M_s s + C_s(s) = M_s s + k_{ds} + k_{ps}/s$, assuming C_m and C_s to be PD controllers.

With respect to stability under time delay, conditions for particular cases of *three-channel* architectures (see Section IV for 3CH architectures) including Z_h and Z_e were previously derived [11]. These architectures, however, fall short of guaranteeing a satisfactory level of transparency. To further explain this problem, a transparency transfer function for the general teleoperation system described by the hybrid model (1) can be defined as $G_{\text{env}} = Z_r/Z_h$, according to Fig. 1. In a 3CH architecture (taking $C_2 = C_6 + 1 = 0$), we have

$$G_{\text{env}} = e^{-2sT} + Z_{ts}(1 - e^{-2sT})/(Z_h C_3). \tag{10}$$

For a large C_3, (10) moves toward e^{-2sT}, which is the ideal condition for transparency in the presence of time delay. On the other hand, the characteristic equation of the transfer function from F_h' to V_m (or any other output in the system) can be calculated as

$$Z_{ts}(e^{2sT} - 1)/C_3 + Z_e e^{2sT} + Z_h = 0. \tag{11}$$

In order to obtain a necessary and sufficient condition for stability based on the Routh–Hurwitz criterion, we use a second-order Padé approximation to rewrite the characteristic equation (11) as

$$(3 - 3sT + s^2T^2)Z_h C_3 + (3 + 3sT + s^2T^2)Z_e C_3 + 6sTZ_{ts} = 0. \tag{12}$$

Assuming $Z_h = M_h s + k_{dh} + k_{ph}/s$ and $Z_e = M_e s + k_{de} + k_{pe}/s$, (12) involves a fourth-order polynomial in s. Application of the Routh–Hurwitz theorem to (12) imposes an upper bound on C_3 that is dependent on time delay T. However, such an upper bound on C_3 for stability limits transparency according to (10). Similarly, taking the 3CH architecture with $C_3 = 0$ would lead to an upper bound on C_2 for stability, which limits transparency according to the transparency transfer function $G_{\text{op}} = Z_t/Z_e$. This fact provides the necessary incentive for extending the concept of passivity-based time delay compensation to the more flexible 4CH teleoperation architecture such that the system can remain stable at no penalty on transparency.

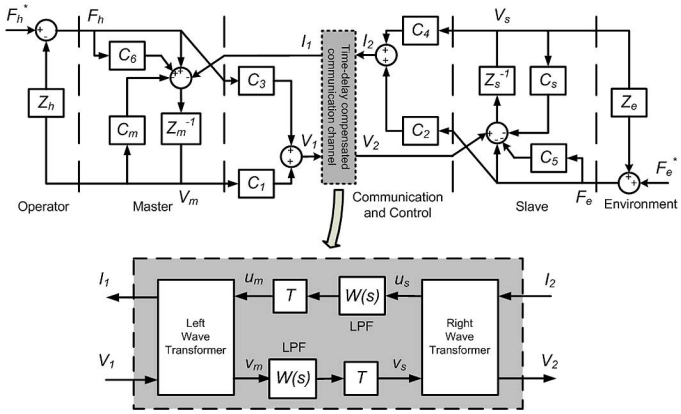

Fig. 3. Passivity-based delay-compensated 4CH teleoperation system.

III. Passivity-Based Delay Compensation in a 4CH Architecture

Thus far, the passivity-based time-delay compensation approach has been applied only to 2CH architectures. In order to extend this approach to a 4CH teleoperation architecture, we need to segregate the communication channel part of the system in Fig. 2 as a two-port network. Fig. 3 shows a possible method for accomplishing this extension, which results in contribution 1) of Section I. The nonphysical input effort and flow pair for this two-port network model of the communication channel in Fig. 3 are

$$V_1 = C_3 F_h + C_1 V_m; \quad I_2 = C_2 F_e + C_4 V_s. \tag{13}$$

The master and the slave closed-loop equations can be written as $V_m Z_m = -V_m C_m + F_h(1 + C_6) - I_1$ and $V_s Z_s = -V_s C_s - F_e(1 + C_5) + V_2$. Therefore, the nonphysical output flow and effort pair are

$$I_1 = F_h(1 + C_6) - V_m Z_{tm}; \quad V_2 = F_e(1 + C_5) + V_s Z_{ts}. \tag{14}$$

The communication channel effort and flow relationships in (13) and (14), from which input and output pseudo-power functions are calculated, are not unique, but in their presented form they are independent of knowledge of Z_e and Z_h, which is an advantage for implementation. The communication channel can be modelled based on its inputs and outputs as

$$\begin{bmatrix} -I_1 \\ V_2 \end{bmatrix} = \begin{bmatrix} c_{11} & c_{12} \\ c_{21} & c_{22} \end{bmatrix} \begin{bmatrix} V_1 \\ I_2 \end{bmatrix} = C(s) \begin{bmatrix} V_1 \\ I_2 \end{bmatrix} \tag{15}$$

where the matrix C can be defined with respect to the hybrid matrix of the communication channel as

$$C(s) = H_{\text{ch}}^{-1}(s) \tag{16}$$

The outputs of the wave transformation block at the master side are

$$I_1 = (\sqrt{2b}u_m - V_1)/b; \quad v_m = (bu_m - \sqrt{2b}V_1)/b \tag{17}$$

and at the slave side

$$V_2 = bI_2 - \sqrt{2b}v_s; \quad u_s = \sqrt{2b}I_2 - v_s. \tag{18}$$

Transformation (17) can be derived from the basic definition of wave variables [i.e., (4)] by taking the flow variable (I_1) and v_m as outputs and the effort variable (V_1) and u_m as inputs. Similarly, wave transformation (18) is obtained from (5) through selecting V_2 and u_s as outputs and I_2 and v_s as inputs. Wave variables v_m and u_s experience time delay T while passing through the communication channel in opposite directions. It can be easily checked that, for the case of $T = 0$, $V_1 = V_2$ and $I_1 = I_2$, thus the original system of Fig. 2 is recovered.

The input/output arrangement in (17) and (18) is due to the fact that the input/output relationship for the communication channel of the proposed 4CH architecture corresponds to an "inverse hybrid" representation of a two-port network (i.e., its inputs are V_1 and I_2 and its outputs are $-I_1$ and V_2, where the directions of the input and output flows corresponds to the convention set in [6])—see (16), whereas that relationship is in the form of a hybrid model for the original 2CH wave-based teleoperation system [7].

A. Absolute Stability Study

In the following theorem, we show that the proposed wave-based 4CH architecture is capable of ensuring absolute stability of the bilateral teleoperation system in the presence of time delay, which results in contribution 2) of Section I.

Theorem 1: Assume that the teleoperation system is coupled to an environment and a human operator, which are both passive but otherwise arbitrary, and define

$$G(s) = \begin{bmatrix} -C_1 Z_{tm}^{-1} & 0 \\ 0 & -C_4 Z_{ts}^{-1} \end{bmatrix}. \tag{19}$$

If $G(s)$ is strictly positive real, then, for any F_h' and F_e' with finite $\mathcal{L}_2$ norms, all of the signals in the system shown in Fig. 3 will have finite norms.

Proof: With the assumption of a passive environment and a human operator, we focus our attention on the portion of the system with F_h and F_e as bounded inputs in Fig. 3. Using (13), (14), and the master and slave closed-loop equations, the 4CH teleoperation system in Fig. 3 can be represented as the single-loop feedback system of Fig. 4, where $G(s)$ and $C(s)$ are defined by (19) and (15), respectively. This feedback system can be subjected to the general passivity theorem [16]. According to this theorem, the conditions for the closed-loop map from input to output to be finite-gain $\mathcal{L}_2$ stable are strict passivity of G and passivity of C.

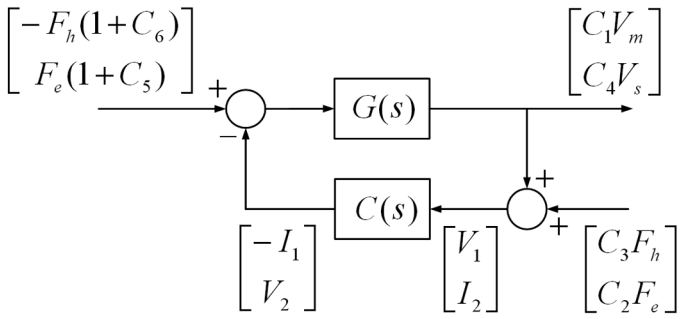

Fig. 4. Simplified single-loop feedback connection of the 4CH teleoperation system.

In order to investigate passivity of the subsystem C, the hybrid matrix of the communication channel (with low-pass filtering) in Fig. 3 is derived as

$$\begin{aligned} h_{11_{\rm ch}} &= \frac{b\left(1 - e^{-2sT}W(s)^2\right)}{e^{-2sT}W(s)^2 + 1} \\ h_{12_{\rm ch}} &= \frac{2e^{-sT}W(s)}{e^{-2sT}W(s)^2 + 1} \\ h_{21_{ch}} &= -\frac{2e^{-sT}W(s)}{e^{-2sT}W(s)^2 + 1} \\ h_{22_{\rm ch}} &= \frac{1 - e^{-2sT}W(s)^2}{b\left(e^{-2sT}W(s)^2 + 1\right)}. \end{aligned} \tag{20}$$

The corresponding scattering matrix for the wave-based communication channel is

$$\begin{aligned} s_{11_{\rm ch}} = s_{22_{\rm ch}} &= \frac{(b^2-1)\left(W^2(s)e^{-2sT} - 1\right)}{(b-1)^2W^2(s)e^{-2sT} - (b+1)^2} \\ s_{12_{\rm ch}} = s_{21_{\rm ch}} &= \frac{-4W(s)be^{-sT}}{(b-1)^2W^2(s)e^{-2sT} - (b+1)^2}. \end{aligned} \tag{21}$$

The singular values for this scattering matrix are given as

$$\sigma_{1,2} = \left|\frac{(b+1)W(s)e^{-sT} \pm (b-1)}{(b-1)W(s)e^{-sT} \pm (b+1)}\right|. \tag{22}$$

Taking $s = j\omega$, the passivity condition $\sigma_1, \sigma_2 \leq 1$, leads to

$$bL^2\omega^2/(1 + L^2\omega^2) \geq 0 \tag{23}$$

which is satisfied as long as $b \geq 0$. Hence, the problem is reduced to passivity analysis of the delay-free transfer matrix G, which depends on the choice of control parameters. Regarding the strict passivity of G, if it has a proper rational form (imposing additional constraints on C_1, C_4, C_m and C_s), strict passivity of G is equivalent to G being strictly positive real [16]. ■

B. Ideal Transparency Requirements

Theorem 1 outlines the condition for absolutely stable operation of the proposed wave-based 4CH architecture with subop-

timal transparency. However, the proposed architecture is flexible enough to also operate with ideal transparency. Applying condition set (9) for ideal transparency without time delay, the overall hybrid parameters of the proposed wave-based 4CH teleoperation system in Fig. 3 are given by

$$\begin{aligned} h_{11} &= (W^2e^{-2sT}-1)\left(Z_{ts}^2 - b^2Z_{tm}^2\right)/D_2 \\ h_{12} &= -h_{21} = 2bWe^{-sT}(Z_{tm}C_3 + Z_{ts}C_2)/D_2 \\ h_{22} &= (W^2e^{-2sT}-1)\left(b^2C_2^2 - C_3^2\right)/D_2 \\ D_2 &= b(W^2e^{-2sT}+1)(Z_{ts}C_2 + Z_{tm}C_3) \\ &\quad + (W^2e^{-2sT}-1)(-b^2C_2Z_{tm} - C_3Z_{ts}). \end{aligned} \tag{24}$$

For asymptotic convergence of the position and torque errors in Fig. 2, controller gains should be chosen in accordance with [15] as

$$C_s/C_m = M_s/M_m. \tag{25}$$

Using (25), it can be easily shown that $Z_{ts}/Z_{tm} = M_s/M_m$. Having h_{11} from (24) equal to zero under ideal transparent condition according to (2) requires

$$b_{\text{ideal}} = Z_{ts}/Z_{tm}. \tag{26}$$

Similarly, for h_{22} to be equal to zero, we should have

$$C_3/C_2 = b_{\text{ideal}}. \tag{27}$$

Using (26) and (27) in (24), expressions for h_{12} and h_{21} under ideal transparency condition can be derived as

$$h_{12} = -h_{21} = W(s)e^{-sT}. \tag{28}$$

Equation (28) means that, for $W(s) = 1$, condition set (9) along with (26) and (27) are ideal transparency provisions for the proposed 4CH architecture of Fig. 3.

In an ideally transparent two-port network under time delay represented by (2), the $\bar{\sigma}$ for the corresponding scattering matrix becomes unbounded [6], which for a reciprocal network this means that the system is not absolutely stable. This deduction is further substantiated by the $G(s)$ in (19), which under the condition set (9) it is easy to show that the corresponding G matrix cannot be strictly positive real. The reason for this is that, due to stability-transparency tradeoff, an ideally transparent teleoperator cannot be stable regardless of the choice of Z_h and Z_e. Indeed, under ideal transparency condition, the delayed 4CH architecture's stability can be shown only if the teleoperation system is terminated with Z_e and the negative feedback through Z_h is also considered in the analysis. In practice, using a low-pass $W(s)$ helps to stabilize the system, although it violates the ideal transparency provisions. However, the cutoff frequency of $W(s)$ establishes a tradeoff between the absolute stability margin of system according to (9), and transparency.

For the teleoperation system under ideal transparency conditions, the input admittance transfer function based on the input F_h' and the output V_m is

$$Y_{\text{in}} = \frac{V_m}{F_h'} = \frac{1 + h_{22}Z_e}{Z_h(1 + h_{22}Z_e) + h_{11} + \Delta_H Z_e} \tag{29}$$

where $\Delta_H = h_{11}h_{22} - h_{12}h_{21}$. Using conditions (26) and (27), the transfer function (29) can be simplified as

$$Y_{\text{in}} = (Z_{ts}C_3)^2/\left[(Z_{ts}C_3)^2(Z_h + Z_e e^{-2sT})\right]. \tag{30}$$

A sufficient condition for Z_{ts} to be Hurwitz is $k_{ds}, k_{ps} > 0$. Having a Hurwitz Z_{ts}, the transfer function (30) can be further simplified to

$$Y_{\text{in}} = \frac{1}{Z_h + Z_e e^{-2sT}}. \tag{31}$$

We investigate stability of the linear time-delay system (LTDS) system represented by (31) in the following theorem, which fulfils contribution 3) of Section I.

Theorem 2: Assuming a mass-spring-damper model for the operator $Z_h = (M_h s^2 + k_{dh}s + k_{ph})/s$, a spring model for the environment $Z_e = k_{pe}/s$, and that the summation matrix $A + A_d$ is Hurwitz, then the LTDS system (31) is asymptotically stable for any delay $T \geq 0$, if there exist matrices $Y > 0$ and $Q > 0$ satisfying

$$A^TY + YA + YA_dQ^{-1}A_d^TY + Q < 0 \tag{32}$$

where

$$A = \begin{bmatrix} 0 & 1 \\ -\frac{k_{ph}}{M_h} & -\frac{k_{dh}}{M_h} \end{bmatrix}; \quad A_d = \begin{bmatrix} 0 & 0 \\ -\frac{k_{pe}}{M_h} & 0 \end{bmatrix}. \tag{33}$$

Proof: In order to conduct the LTDS stability analysis, first the system of (31) has to be described in state space. To this end, taking $x_1 = x_m$ and $x_2 = \dot{x}_m$, $Z_e = k_{pe}/s$, the state-space representation of the system (31) is given by

$$\dot{x}(t) = Ax(t) + A_dx(t - 2T) + Bf_h' \tag{34}$$

where $x = [x_1\ x_2]^T$, $B = [0\ 1/M_h]^T$, and matrices A and A_d are defined according to (33). Expressing the system in this form, its stability for any T can be investigated using [17, Theorem 1]. ∎

Therefore, unlike the passivity framework which addresses the teleoperation system absolute stability, due to stability-transparency tradeoffs, Theorem 2 requires the knowledge of the human operator and environment dynamics for conducting stability analysis under ideal transparent conditions.

In order to present a more descriptive stability analysis of an ideally transparent delayed teleoperation system in terms of interactions among the relevant parameters, it is possible to use Padé approximation to simplify the characteristic polynomial in (31) and apply the Routh–Hurwitz theorem. For mathematical

tractability, we use a first-order Padé approximation $e^{-2sT} \simeq (1-sT)/(1+sT)$ to rewrite the characteristic equation in (31) as

$$M_h T s^3 + (k_{dh}T + M_h)s^2 + (-k_{ph}\alpha T + k_{ph}T + k_{dh})s + k_{ph}\alpha + k_{ph} = 0 \quad (35)$$

where $\alpha = k_{pe}/k_{pm}$. Applying the Routh–Hurwitz theorem to (35), the following condition on α as the necessary and sufficient condition for stability of the system represented by (31) will be derived:

$$\alpha = \frac{k_{pe}}{k_{ph}} < \frac{k_{dh}(M_h + k_{dh}T + k_{ph}T^2)}{k_{ph}(2M_h + k_{dh}T)T}. \quad (36)$$

Equation (36) sets an upper bound on the remote environment stiffness k_{pe} depending on the operator parameters and time delay. Generally speaking, condition (36) is easy to meet particularly under small delays or with compliant environments or through the operator's adaptation to the remote environment characteristics.

IV. 3CH Architecture

Another potential benefit of the general 4CH architecture of Fig. 2, contribution 4) in Section I, is that, by proper adjustment of the local feedback parameters, it is possible to obtain two classes of 3CH control architectures, which can be transparent under delayed ideal conditions. The first class of 3CH architectures is derived by setting $C_2 = 1$ and $C_3 = 0$. As a consequence, $C_5 = -1$ and $C_6 = 0$. In other words, there is no need for master/operator interaction force measurement and therefore, the number of the sensors in the system can be reduced. The second class of 3CH architectures is obtained by setting $C_2 = 0$ and $C_3 = 1$. In this class, force measurement at the slave side is not needed. The need for fewer sensors without imposing additional expense on system transparency makes the 3CH architectures extremely attractive from the implementation point of view.

Deriving a wave-based 3CH architecture from the proposed wave-based 4CH architecture under ideal transparency provisions only affects h_{22} (i.e., force tracking performance remains intact). In order to explain this further, assume under condition set (9) and provisions (25) and (26) that only the slave unity local force feedback is used (i.e., $C_5 = -1$ and $C_6 = 0$). It can be easily shown that h_{11}, h_{12}, and h_{21} still keep their ideal transparency values after this rearrangement. However, the new h_{22} is

$$h_{22} = (W^2 e^{-2sT} - 1)/(2Z_{tm}). \quad (37)$$

According to (37), the bigger the magnitude of Z_{tm}, the closer h_{22} is to its ideal value of zero. This result suggests that this 3CH architecture is suitable for applications in which the master is heavy. On the other hand, if only the master unity local force feedback is used (i.e., $C_6 = -1$ and $C_5 = 0$), while h_{11}, h_{12}, and h_{21} remain unchanged from their ideal transparency values, the new h_{22} is given by

$$h_{22} = -(W^2 e^{-2sT} - 1)/(2Z_{ts}) \quad (38)$$

which shows that the second 3CH architecture is suitable for applications with a heavy slave robot.

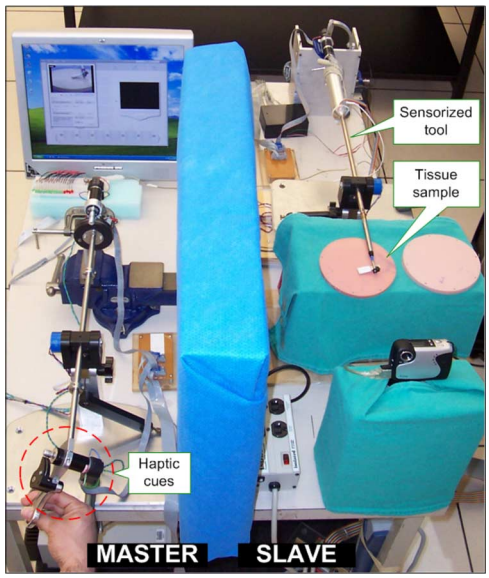

Fig. 5. Master–slave experimental setup.

V. Experimental Results

For experimental performance evaluation, we have used a force-reflective master–slave system developed as an endoscopic surgery test-bed (Fig. 5). Through the master interface, a user controls the motion of the slave surgical tool and receives force/torque feedback of the slave–environment interactions. For details about this master–slave system, the reader is referred to [18]. In the experiments in this paper, the master and slave subsystems were constrained for force-reflective teleoperation in the twist direction only (i.e., rotations about the instrument axis). The user twists the master back and forth, causing the slave to repeatedly probe a soft tissue phantom using a small rigid beam attached to the slave's end-effector (Fig. 5) for about 60 s. The instrument interactions with the tissue are measured and reflected in real time to the user. In the haptic interface, the friction/gravity effects are determined and compensated for such that the user does not feel any weight on his/her hand when the slave is not in contact with an object. The digital control loop is implemented at a sampling frequency of 1000 Hz. The master and the slave effective inertias have been identified to be $M_m = 5.968 \times 10^{-4}$ kgm^2 and $M_s = 9.814 \times 10^{-3}$ kgm^2, respectively.

Fig. 6 shows the master and the slave contact-mode positions and torque tracking profiles for a 4CH wave-based architecture based on the ideal transparency criteria (9), (26), and (27) with single-way time delay $T = 100$ ms, $C_2 = C_3 = 0.5$, $b = 8$, $C_m = 40M_m(10 + s)$ (PD position controller), $C_s =$

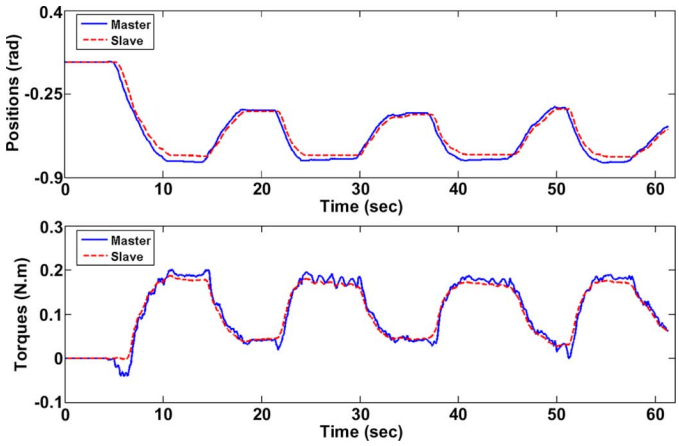

Fig. 6. Position and force tracking profiles for the 4CH wave-based teleoperation architecture with one-way delay $T = 100$ ms.

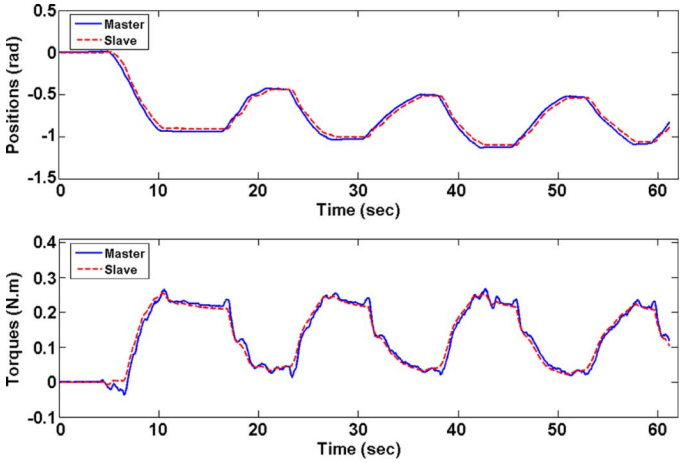

Fig. 7. Position and force tracking profiles for the 3CH wave-based teleoperation architecture with one-way delay $T = 100$ ms.

$40M_s(10 + s)$, and $f_{\text{cut}} = 1$ Hz. Assuming that a dedicated communication network will be used, our choice of one-way time delay of 100 ms is conservative since coast-to-coast round-trip communication delays are expected to be of the order of 60 ms. As shown by the operator torque profile in this figure, the human operator can perceive the environment stiffness through the reflected force and the contact behavior of the system is stable. Fig. 7 shows the same results for a 3CH wave-base architecture with only the unity local force feedback at the slave side (no master local force feedback or $C_6 = 0$ and $C_5 = -1$). All of the other parameters are identical. The reason for choosing this type of 3CH architecture is that in our setup, the slave manipulator is sensorized to measure its interaction force with the environment, while in the absence of a force sensor the master uses a system observer for contact force estimation. Moreover, as reported in [18], master local force feedback $(C_6 \neq 0)$ locally compensates for the user's hand forces, amounting to the user feeling almost zero force when the slave is making contact with a compliant environment. The use of local force feedback at the master side is justifiable only in cases where the user cannot physically overcome the interactions between the slave and the

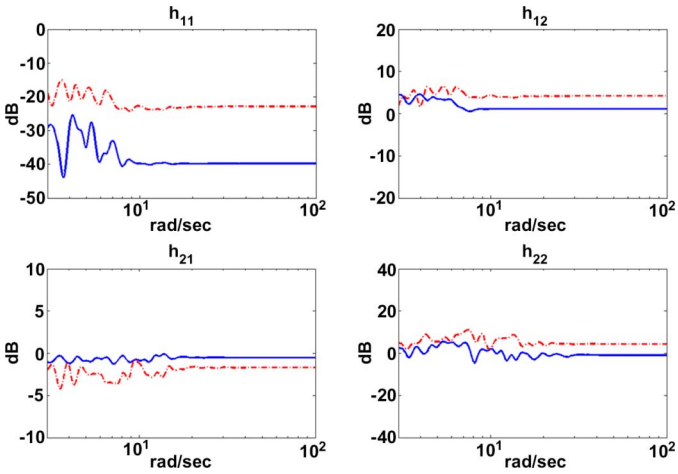

Fig. 8. Magnitudes of the hybrid parameters for the wave-based 4CH and 3CH architectures with one-way delay $T = 100$ ms (dashed line: 4CH; solid line: 3CH).

environment. The contact-mode results in these two figures indicate that the 3CH architecture is better suited for our setup in comparison with the 4CH architecture.

To further investigate the relative transparency of these two systems, a second set of free-motion tests was performed, which in conjunction with the previous contact-mode tests, can be used to determine the hybrid parameters of the teleoperation system in the frequency domain. In the free-motion tests, the master is moved back and forth by the user for about 60 s, while the slave's tip is in free space. Since $f_e = 0$, the frequency response $h_{11} = F_h/X_m$ and $h_{21} = -X_s/X_m$ can be found by applying spectral analysis (MATLAB function *spa*) on the free-motion test data (for the two-port hybrid model based on positions and forces). By using the contact-mode test data, the other two hybrid parameters can be obtained as $h_{12} = F_h/F_e - h_{11}X_m/F_e$ and $h_{22} = -X_s/F_e - h_{21}X_m/F_e$.

The magnitudes of the hybrid parameters of the wave-based 4CH and 3CH teleoperation architectures are shown in Fig. 8. Due to the human operator's limited input bandwidth, these identified hybrid parameters can be considered valid up to a frequency of 60 rad/s. The hybrid parameter $h_{11} = F_h/X_m|_{F_e=0}$ is the input impedance in free-motion condition. Low values of h_{11} are evidence of the fact that when the slave is in free space, the user will feel negligible force thus avoiding a sticky feel of free-motion movements. The parameter $h_{12} = F_h/F_e|_{X_m=0}$ is a measure of force tracking for the haptic teleoperation system. The parameter $h_{21} = -X_s/X_m|_{F_e=0}$ is a measure of the free-motion position tracking performance. The force and free-motion position tracking performance (reflected in the h_{12} and h_{21} spectra of Fig. 8) in the case of the 3CH architecture is almost perfect. The superiority of performance in the case of the 3CH architecture can be attributed to the unity gain of the slave local feedback, which eliminates the master force feedforward (C_3F_h) contribution in the slave side control action and thus, the observation errors do not degrade the control signals. Comparable estimates for h_{22} in the 3CH and 4CH architectures, which is against (37), can be a result of the finite stiffness of the slave and also the backlash present in the slave's gearhead,

which undermine the accuracy of $h_{22} = -X_s/F_e|_{X_m=0}$ estimates. Finally, compared with the traditional 2CH architecture, our results show that the 4CH and 3CH architectures are less susceptible to vibrations under contact conditions [7].

VI. Conclusion

In this paper, we have extended the use of wave theory for time-delay compensation to a 4CH control architecture. The proposed approach is capable of achieving ideal transparency in the presence of time delay. Considering the fact that there is a tradeoff between high transparency and sufficient stability margins, stability of the proposed teleoperation control architecture was rigorously investigated and conditions for both robust stability and stability under ideal transparency were derived. We also studied the 3CH variants of the proposed 4CH control architecture, which present suboptimal transparency in comparison with the optimal case at a lower implementation cost. Finally, we illustrated the developed theory with experimental results obtained using a master–slave setup operating under a 200-ms round-trip time delay.

References

[1] T. B. Sheridan, "Space teleoperation through time delay: Review and prognosis," *IEEE Trans. Robot.*, vol. 9, no. 5, pp. 592–606, Oct. 1993.

[2] B. Hannaford, "A design framework for teleoperators with kinesthetic feedback," *IEEE Trans. Robot. Autom.*, vol. 5, no. 4, pp. 426–434, Aug. 1989.

[3] T. Imaida, Y. Yokokohji, T. Doi, M. Oda, and T. Yoshikawa, "Ground-space bilateral teleoperation of ETS-VII robot arm by direct bilateral coupling under 7-s time delay condition," *IEEE Trans. Robot. Autom.*, vol. 20, no. 3, pp. 499–511, Jun. 2004.

[4] P. Arcara and C. Melchiorri, "Control schemes for teleoperation with time delay: A comparative study," *Robot. Auton. Syst.*, no. 38, pp. 49–64, 2002.

[5] P. F. Hokayem and M. W. Spong, "Bilateral teleoperation: An historical survey," *Automatica*, vol. 42, no. 12, pp. 2035–2057, 2006.

[6] R. J. Anderson and M. W. Spong, "Bilateral control of teleoperators with time delay," *IEEE Trans. Autom. Control*, vol. 34, no. 5, pp. 494–501, Sep. 1989.

[7] G. Niemeyer and J. J. E. Slotine, "Stable adaptive teleoperation," *IEEE J. Oceanic Eng.*, vol. 16, no. 1, pp. 152–162, Jan. 1991.

[8] G. Niemeyer and J. J. E. Slotine, "Telemanipulation with time delays," *Int. J. Robot. Res.*, vol. 23, no. 9, pp. 873–890, Sep. 2004.

[9] D. A. Lawrence, "Stability and transparency in bilateral teleoperation," *IEEE Trans. Robot. Autom.*, vol. 9, no. 5, pp. 624–637, Oct. 1993.

[10] Y. Yokokohji and T. Yoshikawa, "Bilateral control of master-slave manipulators for ideal kinesthetic coupling-formulation and experiment," *IEEE Trans. Robot. Autom.*, vol. 10, no. 5, pp. 605–619, Oct. 1994.

[11] K. Hashtrudi-Zaad and S. E. Salcudean, "Transparency in time delay systems and the effect of local force feedback for transparent teleoperation," *IEEE Trans. Robot. Autom.*, vol. 18, no. 1, pp. 108–114, Feb. 2002.

[12] N. A. Tanner and G. Niemeyer, "High-frequency acceleration feedback in wave variable telerobotics," *IEEE/ASME Trans. Mechatronics*, vol. 11, no. 2, pp. 119–127, Apr. 2006.

[13] J. E. Colgate, "Robust impedance shaping telemanipulation," *IEEE Trans. Robot. Autom.*, vol. 9, no. 4, pp. 374–384, Jun. 1993.

[14] S. Yamamoto and H. Kimura, "On structured singular values of reciprocal matrices," in *Proc. Amer. Control Conf.*, 1995, pp. 3358–3359.

[15] M. Tavakoli, R. V. Patel, and M. Moallem, "Bilateral control of a teleoperator for soft tissue palpation: Design and experiments," in *Proc. IEEE Int. Conf. Robot. Autom.*, 2006, pp. 3280–3285.

[16] H. K. Khalil, *Nonlinear Systems*, 3rd ed. Upper Saddle River, NJ: Prentice-Hall, 2002.

[17] J. Zhang, C. R. Knopse, and P. Tsiotras, "Stability of time-delay systems: Equivalence between Lyapunov and scaled small-gain conditions," *IEEE Trans. Autom. Control*, vol. 46, no. 3, pp. 482–486, Mar. 2001.

[18] M. Tavakoli, R. V. Patel, and M. Moallem, "A haptic interface for computer-integrated endoscopic surgery and training," *Virtual Reality*, no. 9, pp. 160–176, 2006.